pp 22–41.
doi:10.1017/aer.2020.82

Research on the design of smart morphing long-endurance UAVs

T. Ma
matielin@buaa.edu.cn
Beijing Advanced Subject Center of Advanced Unmanned Aerial Vehicles
Key Laboratory of Advanced Technology of Intelligent Unmanned Flight System
Ministry of Industry and Information Technology
Institute of Unmanned System
Beihang University
Beijing
China

Y. Liu
School of Aeronautic Science and Engineering
Beihang University
Beijing
China

D. Yang
tornado831001@hotmall.com
SATM
Cranfield University
Cranfield
UK

Z. Zhang and **X. Wang**
School of Aeronautic Science and Engineering
Beihang University
Beijing
China

S. Hao
School of Aeronautic Science and Engineering
Hiwing General Aviation Equipment Co. LTD
Beihang University
Beijing
China

ABSTRACT

To improve the endurance performance of long-endurance Unmanned Aerial Vehicles (UAVs), a smart morphing method to adjust the UAV and flight mode continuously during

Received 30 December 2019; revised 5 August 2020; accepted 12 August 2020.

flight is proposed. Using this method as a starting point, a smart morphing long-endurance UAV design is conducted and the resulting improvement in the endurance performance studied. Firstly, the initial overall design of the smart morphing long-endurance UAV is carried out, then the morphing form is designed and various control parameters are selected. Secondly, based on multi-agent theory, an architecture for the smart morphing control system is built and the workflow of the smart morphing control system is planned. The morphing decision method is designed in detail based on the particle swarm optimisation algorithm. Finally, a simulation of the smart morphing approach in the climb and cruise stages is carried out to quantitatively verify the improvement in the endurance performance. The simulation results show that the smart morphing method can improve the cruise time by 4.1% with the same fuel consumption.

Keywords: Smart morphing; Long-endurance UAV; Endurance; Fuel consumption

NOMENCLATURE

a_x	acceleration in x-axis direction
a_z	acceleration in z-axis direction
a_0	angle-of-attack at zero lift
A	wing aspect ratio
C	specific fuel consumption
c	relative thickness of wing
C_D	whole UAV drag coefficient
C_{D0}	drag coefficient at zero lift
C_{Di}	induced drag coefficient
C_{Power}	fuel consumption per unit power per hour
C_y	UAV lift coefficient
C^a_{yswing}	wing slope of lift curve
C^a_{foil}	aerofoil slope of lift curve
C^a_{yhtail}	horizontal tail slope of lift curve
C^a_{fhtail}	horizontal tail aerofoil slope of lift curve
C_{ywing}	wing lift coefficient
C_{yhtail}	horizontal tail lift coefficient
D	drag
E	endurance
L/D	lift-to-drag ratio
P	engine output power
S_W	reference wing area
s_{ht}	reference horizontal wing area
$s_{fuselage}$	reference fuselage area
S	fuel consumption per hour
T	thrust produced by engine
V	speed

https://doi.org/10.1017/aer.2020.82 Published online by Cambridge University Press

V_y	climb rate
W	weight
W_i	weight before cruise
W_f	weight after cruise
x	x coordinate of mean camber line
Z_x	Z coordinate of mean camber line
$\triangle thTE$	thickness of trailing edge

Greek Symbols

α	angle-of-attack
γ	angle-of-climb
φ	incidence angle
ρ	atmospheric density
η	engine efficiency
ε	downwash angle
η_p	engine efficiency

1.0 INTRODUCTION

Long-endurance UAVs play an important role in the military arsenal. They can perform reconnaissance and surveillance missions in high-threat environments without risking pilot lives[1]. Improving their endurance performance enhances their combat capabilities and has always been a research focus in the field of long-endurance UAV design.

With the rapid development of Artificial Intelligence (AI) and morphing technology, the concept of smart morphing aircraft has been proposed. Smart morphing implies that the aircraft is self-sensing and has an adaptive control ability. The aircraft can thus change shape in a timely and autonomous fashion depending on the flight task and flight environment, thus meeting different flight requirements with different wing geometries and achieving optimised performance across the entire flight envelope[2,3].

The design of such smart morphing control system architectures and planning the corresponding workflow must be considered during the design of smart morphing long-endurance UAVs. The smart morphing process involves environment perception, morphing decision-making and maintaining the trim of the UAV. Multi-agent theory in the field of AI provides a new design approach for the architecture of such smart morphing control systems. A multi-agent system refers to an agent network consisting of several autonomous, flexible and social computer systems operating in a certain cooperative mode. Yin et al.[4] designed an intelligent control system framework for the chassis of an electric vehicle based on multi-agent theory to realise multi-objective online optimal regulation and control of the vehicle under different conditions. Similarly, multi-agent theory can be used to design smart morphing control systems. At the same time, a learning agent can be added to realise independent learning of the smart morphing control system.

The term ‘smart’ in smart morphing mainly refers to the adjustment of the aircraft configuration and flight operation according to the flight environment. Therefore, how to select the optimal shape according to the current environment is the emphasis during the design

https://doi.org/10.1017/aer.2020.82 Published online by Cambridge University Press

of such smart morphing control systems. The use of an appropriate optimisation algorithm can shorten the decision time and improve the decision efficiency. Particle swarm optimisation has been proposed as an intelligent algorithm to imitate the foraging behaviour of birds[5]. Anlinxue et al.[6] compared the particle swarm optimisation algorithm with the genetic algorithm and sequential quadratic programming algorithm, finding that the particle swarm optimisation algorithm exhibited better global search capability and higher efficiency. Therefore, smart morphing decision-making can be designed based on particle swarm optimisation.

The 'morphing' in smart morphing, in contrast to the traditional control surface deflection of the wing, refers to continuous deformation of the wing[2], mainly by variation of its camber, span and sweep angle. Among these, camber is the main factor generating the lift force of the wing. Changing the camber can improve the flow field and effectively improve the aerodynamic performance. The use of wings with variable camber has thus become the focus of both domestic and foreign research. In recent years, the development of shape memory materials such as piezoelectric materials and other intelligent materials has provided a good materials basis for such variable-camber wings. Elzey et al.[7] at the University of Virginia used a shape memory alloy to design a chain-link-type variable-camber wing with a large range of bending deformation. Wu et al.[8] presented a new morphing aerofoil design concept that combines compliant runners driven by Linear Ultrasonic Motors (LUSMs) with an innovative morphing structure using a compliant composite truss. This approach can offer fully controlled multiple degrees of freedom to provide multiple morphing configurations. Guiler et al.[9] conducted wind-tunnel tests, and the results showed that, in comparison with a traditional wing with flaps, the variable-camber wing that deformed smoothly across the wing surface exhibited a 15% higher lift-to-drag ratio while its resistance was reduced by 7%. Therefore, the morphing form of variable camber can be selected.

In this paper, the morphing form of variable camber is selected, and a preliminary design for a smart morphing long-endurance UAV is completed. The design work includes the overall parameter and aerodynamic layout, morphing, the smart morphing control system architecture and finally the morphing decision method. The effects of such smart morphing on the endurance are verified by simulating the UAV in climb and cruise flight.

2.0 SMART MORPHING CONTROL SYSTEM ARCHITECTURE BASED ON MULTI-AGENT THEORY

The common multi-agent architecture includes an agent alliance, agent network and blackboard structure. Information sharing between the individual agents is realised through the blackboard structure[10], which is used herein as the basis for the design of the architecture of the smart morphing control system and to plan the operation of the smart morphing control system.

The smart morphing control system is composed of a bulletin board, a perception and detection agent, a morphing decision agent and a balance control agent, as shown in Fig. 1. Each agent is an independent computing entity with knowledge, belief, commitment, ability etc. Each agent shares information and cooperates with the other agents through the bulletin board.

The perception and detection agent can obtain data from the sensor network that extends all over the UAV and has the ability for information fusion. The data obtained from the sensor network can be used for state and parameter estimation. The information obtained by the

https://doi.org/10.1017/aer.2020.82 Published online by Cambridge University Press

Table 1
The information obtained by the perception and detection agent

Environment information	Flight information	UAV state
Flight altitude	Flight path angle	Current weight
Wind speed	Angle-of-attack	Engine state
. . .	Flight speed	Morphing state
	Acceleration	. . .
	. . .	

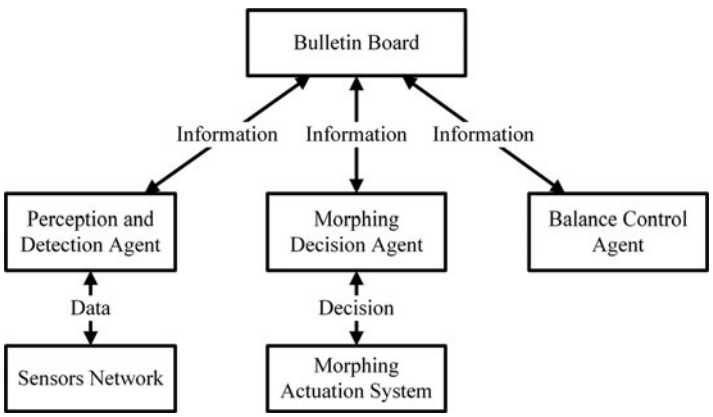

Figure 1. Smart morphing control system architecture.

perception and detection agent can then be transmitted to the bulletin board. Table 1 lists the information obtained by the perception and detection agent by fusing the information transmitted by the sensor network.

The bulletin board publicises the flight tasks and the information obtained from the perception and detection agent to the other agents and receives the information from all the agents.

According to the information on the bulletin board, the morphing decision agent decides the optimal shape and flight mode, aiming to improve the endurance, and also has the ability for autonomous learning. Figure 2 shows the architecture of the morphing decision agent. Figure 3 shows the workflow of the morphing decision agent, which includes a database, learning sub-agent and decision-making sub-agent. The database contains previous flight data and relevant flight knowledge, which can be updated in real time. According to the current state, the decision-making sub-agent makes the morphing decision and the corresponding flight mode. The learning sub-agent learns the decisions through the neural network algorithm, and constructs and updates the decision prediction model. After learning a considerable number of flight data, the decision prediction model can replace the decision-making sub-agent.

The balance control agent considers the flight mode decision made by the morphing decision agent as a reference and adjusts the aircraft according to the information given on the bulletin board to ensure flight stability.

The whole operating process of the smart morphing control system is shown in Fig. 4.

https://doi.org/10.1017/aer.2020.82 Published online by Cambridge University Press

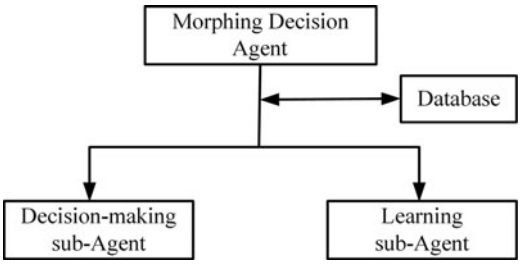

Figure 2. The morphing decision agent architecture.

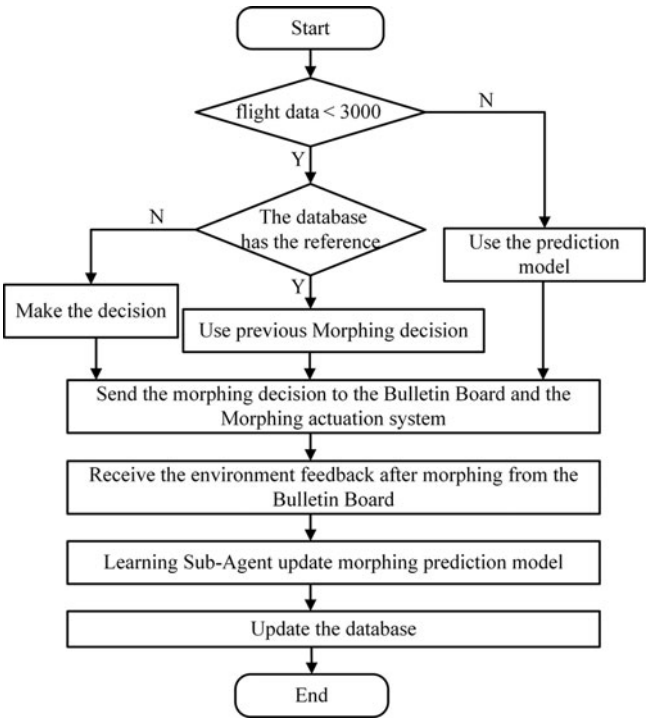

Figure 3. The workflow of the decision-making sub-agent.

3.0 THE DESIGN OF THE SMART MORPHING LONG-ENDURANCE UAV

A smart morphing long-endurance UAV is designed in this section. The configuration layout is based on the existing long-endurance General Atomic MQ-1 'Predator UAV', and the morphing wing is designed in detail.

3.1 The concept design

The main flight parameters of the smart morphing long-endurance UAV are presented in Table 2, while the flight profile is shown in Fig. 5.

https://doi.org/10.1017/aer.2020.82 Published online by Cambridge University Press

Table 2
Flight parameters of the smart morphing long-endurance UAV

Name	Value	Unit
Operational ceiling	7.5	km
Cruise speed	144–180	km/h
Stall speed	100	km/h
Max. speed	216	km/h
Total weight	1020	kg
Empty weight	500	kg

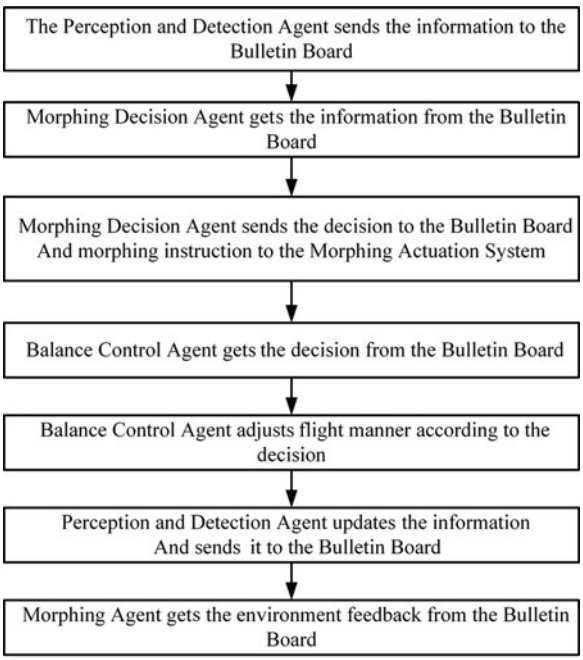

Figure 4. The smart morphing control system workflow.

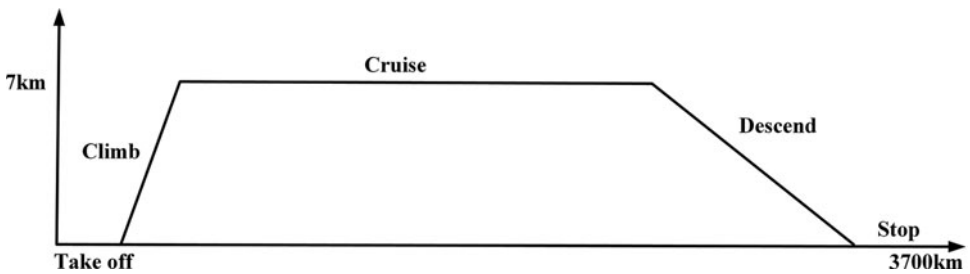

Figure 5. The smart morphing long-endurance UAV flight profile.

https://doi.org/10.1017/aer.2020.82 Published online by Cambridge University Press

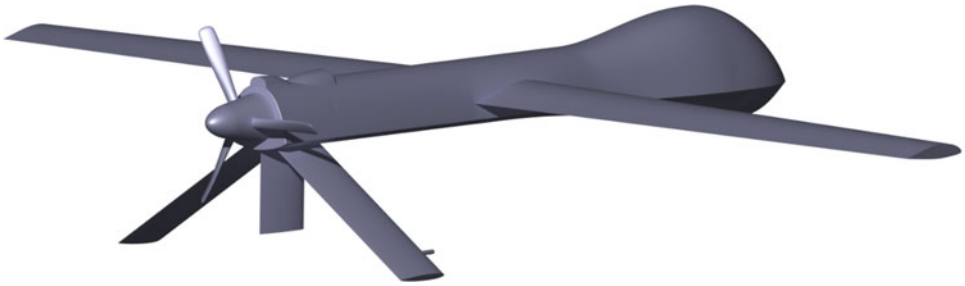

Figure 6. The configuration layout of the smart morphing long-endurance UAV.

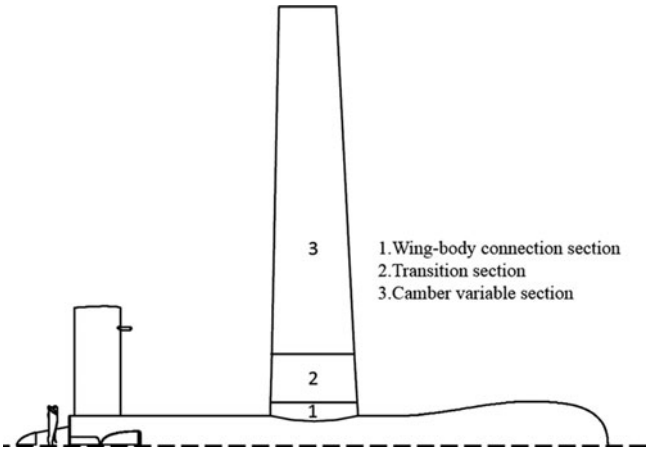

Figure 7. The morphing wing distribution.

3.2 Configuration layout design

A single 115-hp Rotax 914F/UL turbo-charged four-cylinder engine powers the UAV, and a large-aspect-ratio wing is adopted to reduce the induced drag with an inverted V-shaped tail to avoid the influence of the flow of the wing. The Three-Dimensional (3D) configuration layout of the smart morphing long-endurance UAV is shown in Fig. 6.

3.3 Morphing design

The morphing bends the trailing edge of the wing to change the wing camber while leaving the thickness distribution unchanged. The distribution of the morphing wing is shown in Fig. 7. Along the span length, it is divided into the wing–body connection section, the transition section and the camber-variable section. The camber-variable section accounts for 80% of the wing span. The morphing is uniform along the span.

The morphing structure is designed with reference to HongDa Lis article[15]. The details of the morphing wing are shown in Fig. 8. The transition section uses a flexible skin. One end is the rigid wing rib, while the other end is the morphing structure. The morphing structure includes the rigid structure, the driving skin (which is mainly made of shape memory alloy), the flexible baseplate that is fixed to the rigid structure and can be deformed by the driving skin, and the artificial muscles, which are used to hold the flexible baseplate in place.

https://doi.org/10.1017/aer.2020.82 Published online by Cambridge University Press

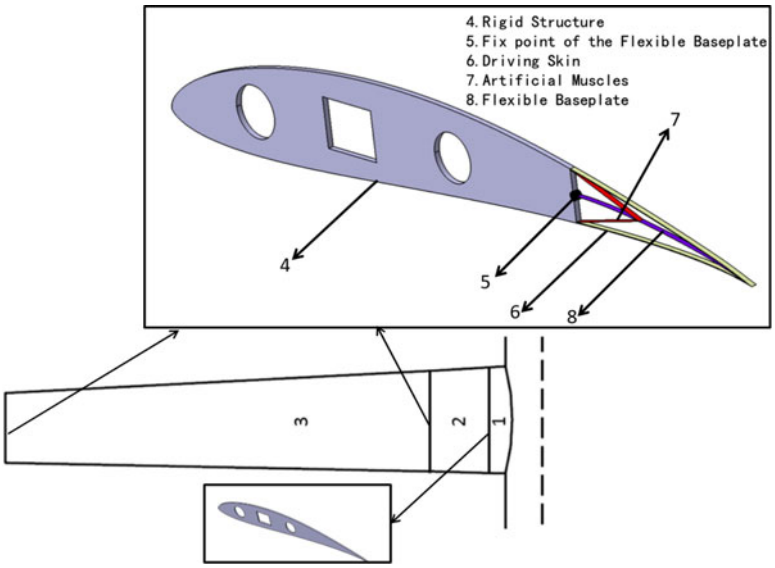

Figure 8. The morphing wing design.

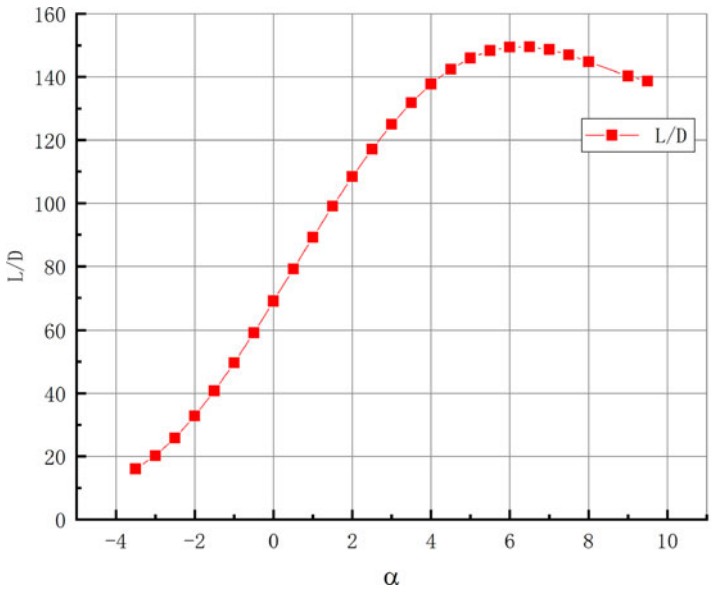

Figure 9. The L/D of the original aerofoil.

Thus, by controlling the driving skin, the morphing structure can change the trailing edge on demand.

The maximum thickness of the initial aerofoil is 13%, distributed at 32.5% of the aerofoil chord. The relative camber is 4.93% at 30% of the aerofoil chord. The lift-to-drag ratio of this aerofoil at the cruise Reynolds number is shown in Fig. 9. The maximum L/D of this aerofoil occurs at 6.5 where its lift coefficient is equal to 1.327. The lift coefficient required for cruise

https://doi.org/10.1017/aer.2020.82 Published online by Cambridge University Press

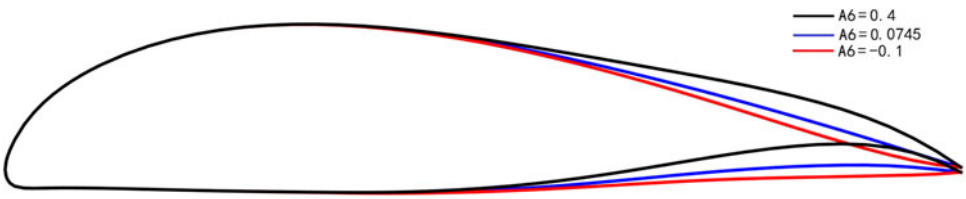

Figure 10. The aerofoil change range.

is about 1.32, so this aerofoil is selected as the original aerofoil because of its maximum L/D at the cruise lift coefficient.

The unit chord aerofoil was parametrised using the CST parametrisation method, based on the expression[11]

$$Z(x) = x^{N1}(1-x)^{N2}\sum_{i=0}^{n} A_i S(x)_i + 0.5x \triangle thTE. \quad \ldots (1)$$

where $\sum_{i=0}^{n} A_i S(x)_i$ is the shape function, $Z(x)$ is the Z coordinate of the mean camber line, $N1$ and $N2$ determine the shape of the aerofoil (for this aerofoil, $N1 = 0.5$ and $N2 = 1$) and A_i are the control parameters. The sixth-order Bernstein function is adopted as the shape function, that is, $n = 6$, thus A0–A6 are introduced as seven control parameters to control the upper and lower wing surfaces. Among these, the change of the sixth control parameter A6 on the leading edge of the aerofoil is small and can be ignored. It can be used as a control parameter for the shape of the trailing edge. By changing the value of the sixth parameter A6 of the mean camber line expression while maintaining the same thickness distribution, bending the trailing edge to change the camber without changing the thickness can be simulated. The sixth parameter A6 corresponding to the initial aerofoil mean camber line is 0.0745. To ensure the rationality of the aerofoil change, A6's change range is set as [–0.1, 0.4], and the corresponding aerofoil change range is shown in Fig. 10.

4.0 MORPHING DECISION-MAKING METHOD FOR SMART MORPHING LONG-ENDURANCE UAV DESIGN

To simulate the variation of the smart morphing long-endurance UAV during flight, appropriate models should be established. Meanwhile, the morphing decision-making method has to be designed for the morphing decision agent. The simulation then operates based on these models and the designed method.

4.1 Balance equation, aerodynamic model and engine model

4.1.1 Balance equation

The balance equations in the climb stage are as follows:

$$T\sin\alpha + L = W\cos\gamma + ma_x, \quad \ldots (2)$$

https://doi.org/10.1017/aer.2020.82 Published online by Cambridge University Press

$$T\cos\alpha - D = W\sin\gamma + ma_x. \quad \ldots(3)$$

The balance equations in the cruise stage are as follows:

$$T\sin\alpha + L = W, \quad \ldots(4)$$

$$T\cos\alpha - D = ma_x. \quad \ldots(5)$$

4.1.2 Aerodynamic model

According to the 'Aerodynamics Manual', the lifting coefficient of a high-aspect-ratio aircraft can be calculated using Equation (7), assuming that the contribution of the fuselage to the lift is negligible. In this article, the wing has no twist. Thus, the whole UAV lift calculation model is established as Equation (8). The coefficients C^{α}_{yswing} and C^{α}_{yhtail} can be calculated from the aerofoil correlation coefficient using Equations (9) and (10), assuming an elliptical lift distribution. Meanwhile, the downwash angle can be calculated using Equation (11)[16].

$$L = O.5\rho V^2 S_W C_y, \quad \ldots(6)$$

$$C_y = C^{\alpha}_{yswing}(\alpha - \alpha_0) + C^{\alpha}_{yhtail}(1-\varepsilon)\alpha\frac{s_{ht}}{S_W}, \quad \ldots(7)$$

$$C_y = C^{\alpha}_{yswing}(\alpha - \alpha_0) + 0.183C^{\alpha}_{yhtail}(1-\varepsilon)\alpha, \quad \ldots(8)$$

$$C^{\alpha}_{yswing} = \frac{C^{\alpha}_{foil}}{1 + 1.5\frac{C^{\alpha}_{foil}}{\pi A}}, \quad \ldots(9)$$

$$C^{\alpha}_{yhtail} = \frac{C^{\alpha}_{fhtail}}{1 + 1.5\frac{C^{\alpha}_{fhtail}}{\pi A}}, \quad \ldots(10)$$

$$\varepsilon = 0.159\frac{C^{a}_{yswing}}{C^{\alpha}_{foil}}. \quad \ldots(11)$$

The drag coefficient of a high-aspect-ratio aircraft is calculated using Equation (13). C_{D0} is divided into the wing drag coefficient at zero lift C_{D0wing} and the fuselage drag coefficient at zero lift $C_{D0fuselage}$ as shown in Equation (14). C_{D0wing} is calculated using Equation (15). C_{Di} can be calculated using Equation (16), and K_1 and K_2 are empirical coefficients. The whole UAV C_{D0} and C_{Di} can be calculated using Equations (17) and (18)[16].

$$D = O.5\rho V^2 S_W C_D, \quad \ldots(12)$$

$$C_D = C_{D0} + C_{Di}, \quad \ldots(13)$$

$$C_{D0} = C_{D0wing} + C_{D0fuselage}\frac{s_{fuselage}}{S_W}, \quad \ldots(14)$$

https://doi.org/10.1017/aer.2020.82 Published online by Cambridge University Press

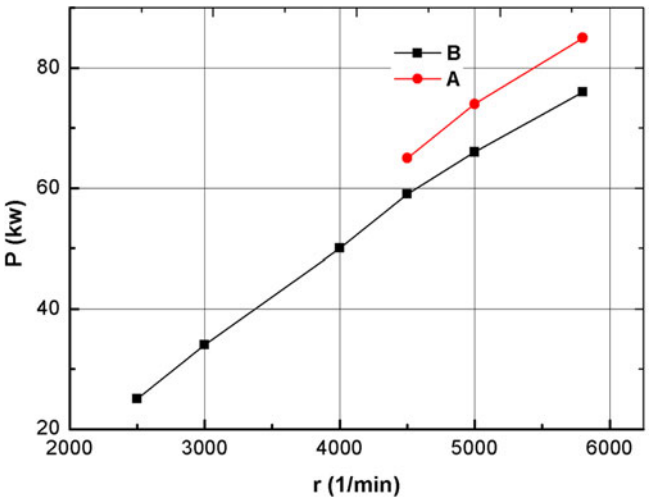

Figure 11. Change of engine output power with RPM.

$$C_{D0wing} = 2(1 + 1.44c + 2c^2)\,(1 - 0.09\mathrm{M}^2), \quad \ldots (15)$$

$$C_{Di} = K_1 C_{yswing}^2 + K_2 C_{yhtail}^2, \quad \ldots (16)$$

$$C_{D0} = 0.0100633 + 0.0092(1 - 0.09\mathrm{M}^2), \quad \ldots (17)$$

$$C_{Di} = 0.936\frac{C_{yswing}^2}{47.91} + 0.183\frac{C_{yhtail}^2}{20.7}. \quad \ldots (18)$$

The aerofoil's aerodynamic coefficient data were generated using Xfoil for various cambers and flight Mach and Reynolds numbers. The invariable setting used in Xfoil is an 'Ncrit' value of 9, due to its very good correlation with experiment according to research on the eN method of transition prediction by Smith and Gambeoni[17]. The Reynolds and Mach number settings change with the flight conditions.

4.1.3 Engine model

The variation of the output power of the ROTAX 914F/UL engine with RPM is shown in Fig. 11[12]. The relationship between the RPM and fuel consumption is shown in Fig. 12[12], where A indicates the engine take-off state and B the engine continuous throttle performance. The change in the output power of the engine with altitude is shown in Fig. 13[12]. The relationship between the fuel consumption rate s (L/h) and the output power P is obtained as follows:

$$s = 10.566 + 0.26P(\mathrm{A}), \quad \ldots (19)$$

$$s = 5.199 + 0.29P(\mathrm{B}). \quad \ldots (20)$$

https://doi.org/10.1017/aer.2020.82 Published online by Cambridge University Press

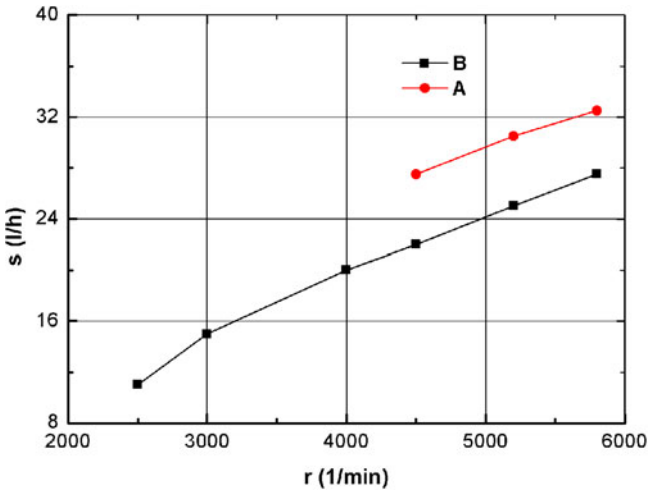

Figure 12. Change of fuel consumption with RPM.

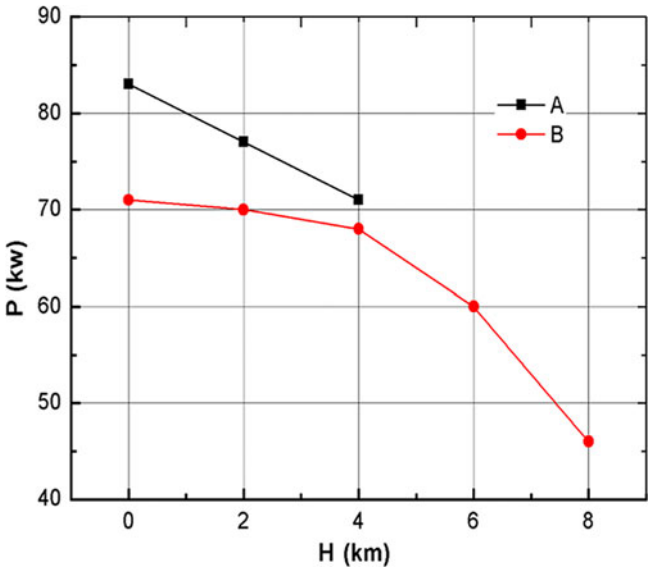

Figure 13. Change of engine output power with altitude.

4.2 Decision-making method

In the decision-making process, the particle swarm optimisation algorithm is adopted, the weight factor is 0.8 and both learning factors are set to 1.5. The decision-making process is shown in Fig. 14. First, the original particle swarm is obtained, then the location of each particle is adjusted one by one according to the force balance constraint. Second, the fitness of each particle is calculated using the model established in this article, to determine the best

https://doi.org/10.1017/aer.2020.82 Published online by Cambridge University Press

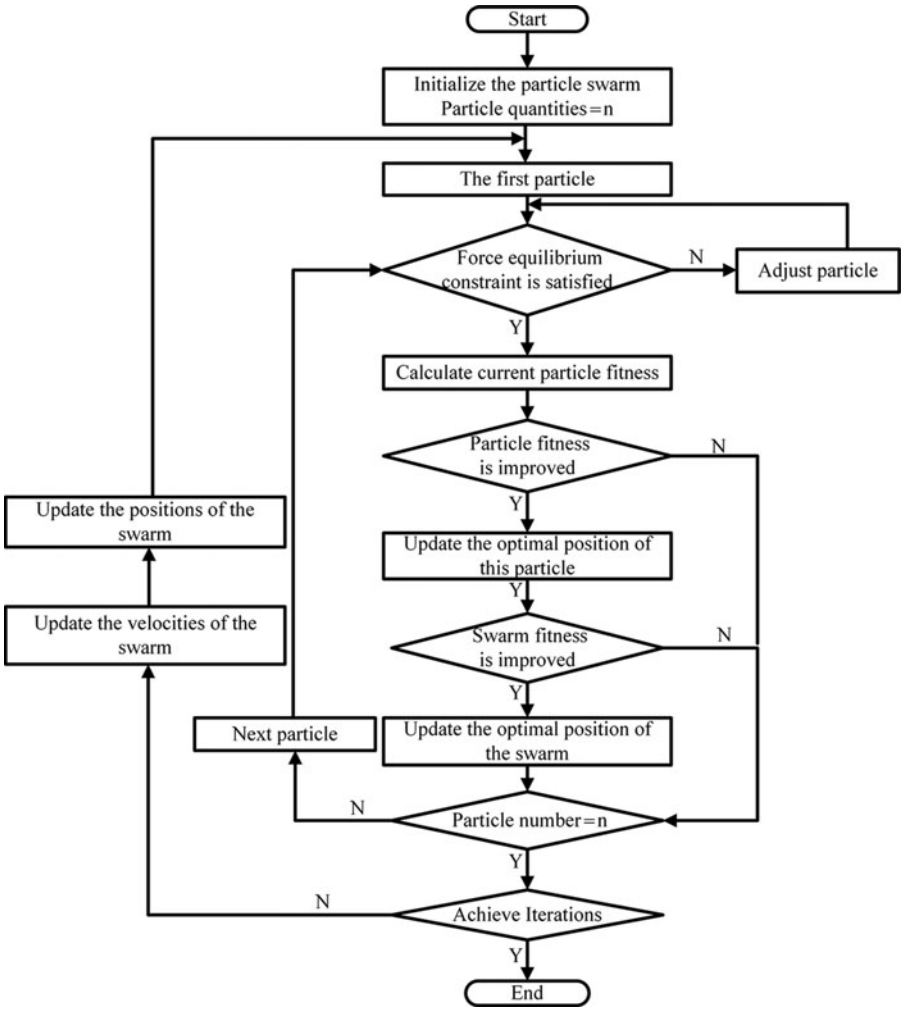

Figure 14. Morphing decision method.

fitness of the original particle swarm and the best fitness of each particle. The location of each particle is then changed according to the location of the particle with the best particle swarm fitness and the past location corresponding to the best-ever fitness of that particle. Then, the above steps are repeated until the prescribed number of iterations is reached. Throughout this process, the smart flight operation can be simulated by adjusting the UAV shape, the angle-of-attack α and the flight speed V according to the flight environment.

4.3 Decision objectives

The purpose of the climb stage is to climb to the cruise altitude rapidly. Therefore, the morphing decision-making goal in the climb stage is to maximise the rate of climb, expressed as follows: $\mathrm{Max}(V_y)$.

https://doi.org/10.1017/aer.2020.82 Published online by Cambridge University Press

During the cruise stage, the 'instantaneous endurance' and the endurance E are calculated as follows; the morphing decision-making goal in the cruise stage is to maximise the endurance E:

$$\frac{dE}{dW} = -\frac{1}{CT} = -\frac{n_p}{C_{Power}VT}, \quad \ldots(21)$$

$$E = \int_{W_i}^{W_f} -\frac{1}{CT} dw. \quad \ldots(22)$$

5.0 SMART MORPHING SIMULATION AND STUDY ON ENDURANCE IMPROVEMENT

Smart morphing simulations are carried out in the climb and cruise flight stages to study the improvement effect of smart morphing on endurance.

5.1 Flight process simulation

In the climb stage, the true airspeed corresponding to the maximum climb rate changes with altitude. For the smart morphing long-endurance UAV designed herein, the climb stage starts at 0km with a flight speed of 127.8km/h and the climb altitude is 7km. During the whole climb stage, the engine is working at its maximum output power condition.

In the cruise stage, the smart morphing long-endurance UAV cruises at the same altitude of 7km but with a variable angle-of-attack, speed and shape parameter A6, to achieve the goal of maximum endurance (14).

The initial weight of the long-endurance UAV is 1020kg, and the available fuel for the two stages is 220kg.

5.2 Smart morphing simulation

In the climb stage, the main variable parameter is the flight altitude. Therefore, the smart morphing simulation is carried out for every kilometre of altitude. The smart morphing objective is to maximise the climb rate, while the decision factors are the aerofoil shape control parameter A6 and the flight angle-of-attack α. The changes of the aerofoil parameter A6 and the angle-of-attack α during climb are shown in Fig. 15. The corresponding change in the flight speed V is shown in Fig. 16. Figure 15 shows that, with increasing flight altitude, the optimal angle-of-attack α and the aerofoil shape control parameter A6 change with altitude regularly and obviously. With increasing altitude, the optimal climb mode exhibits a continuously reduced angle-of-attack and increased shape control parameter A6.

The main parameter varying during the cruise stage is weight, and the smart morphing decision-making simulation is carried out for every 20kg of fuel consumed. The smart morphing objective is to minimise the fuel consumption per unit time, s. The decision factors are the aerofoil shape control parameter A6, the angle-of-attack α and the flight speed V. The variation of the aerofoil shape parameter A6 and the angle-of-attack α with the UAV weight is shown in Fig. 17. The corresponding change of flight speed is shown in Fig. 18. It can be seen that, during the cruise stage, with the consumption of fuel, the optimal cruise mode is to reduce the aerofoil shape parameter A6, angle-of-attack α and flight speed V continuously. Compared with the climb stage, the variation of the aerofoil shape control parameter A6 and the angle-of-attack α during the cruise stage is smaller because the weight change has

https://doi.org/10.1017/aer.2020.82 Published online by Cambridge University Press

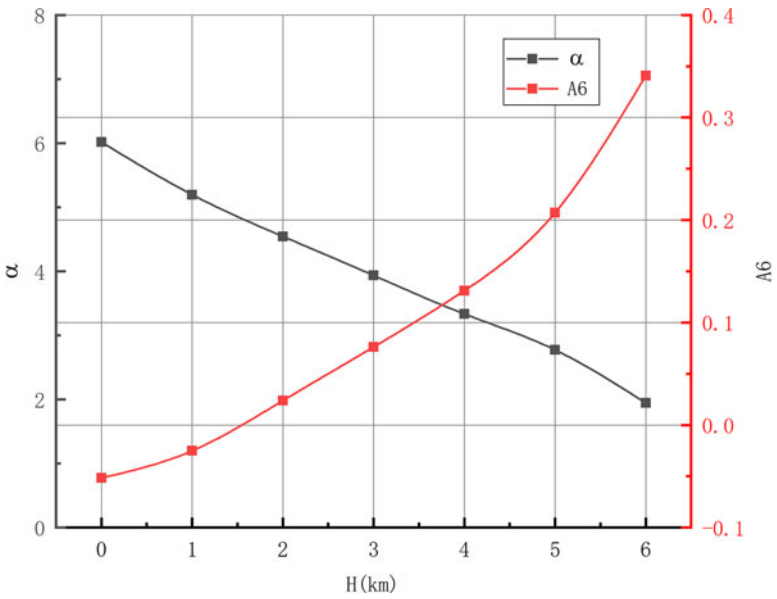

Figure 15. Changes of the aerofoil shape parameter A6 and the angle-of-attack α with altitude in the climb stage.

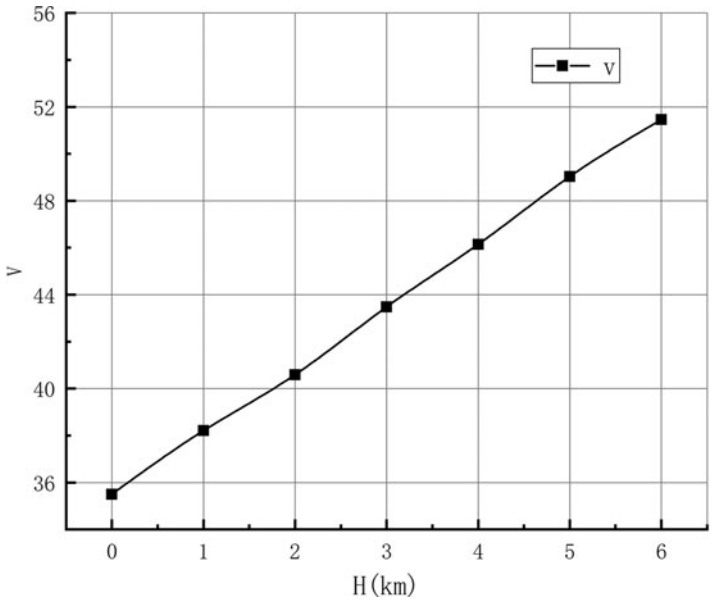

Figure 16. Corresponding change of flight speed with altitude in the climb stage.

less impact than the altitude. Also, the value of A6 needed for improving endurance is also larger than during the climb stage. This occurs because reducing the drag can improve the endurance, so the larger A6 is, the less camber the aerofoil has, which means that C_{Di} can be reduced.

https://doi.org/10.1017/aer.2020.82 Published online by Cambridge University Press

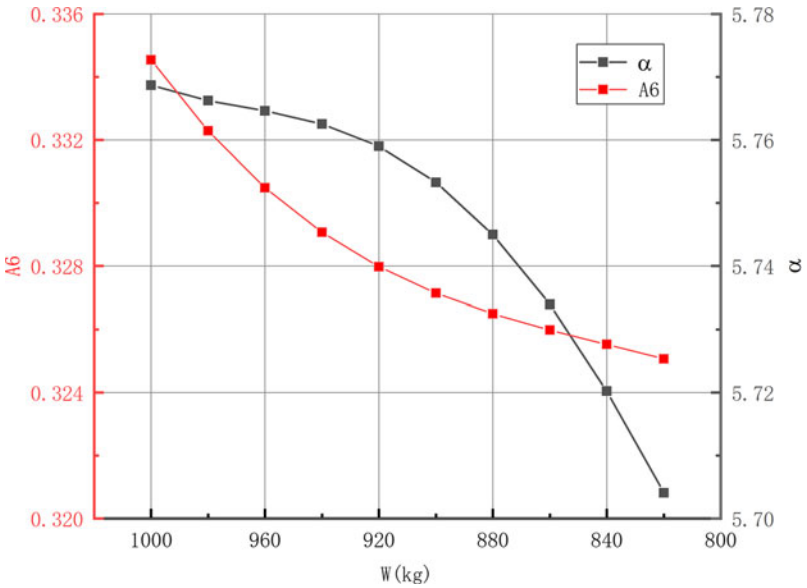

Figure 17. Changes of A6 and α with weight in the cruise stage.

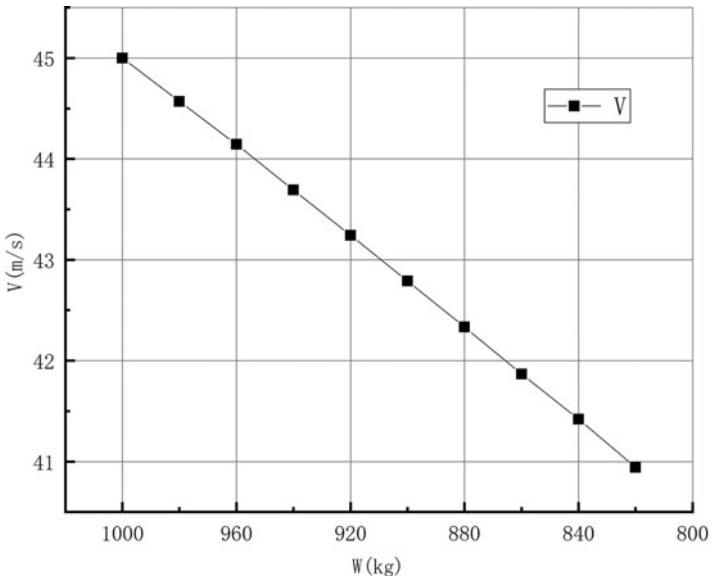

Figure 18. Change of V with weight in the cruise stage.

5.3 Smart morphing effect on endurance improvement

The climb rate V_y of the smart morphing long-endurance UAV is compared with the climb rate V_{y0} of the long-endurance UAV without smart morphing technology in Fig. 19, revealing an increase in the average climb rate by about 0.16%. The fuel consumption rate of the engine

https://doi.org/10.1017/aer.2020.82 Published online by Cambridge University Press

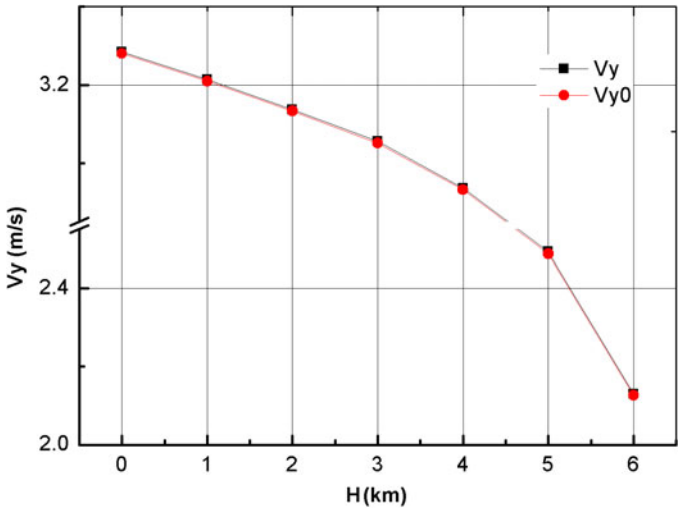

Figure 19. Change of the smart morphing long-endurance UAV climb rate with altitude compared with the long-endurance UAV without smart morphing.

in the climb stage is 20.625kg/h. The total fuel consumption in the climb stage is calculated as follows, where V_y is calculated at every 1km of altitude:

$$\triangle W = \sum_{i=1}^{7} \triangle W_i = \sum_{i=1}^{7} \frac{20.625}{V_y}. \quad \ldots (23)$$

The calculation shows that, in the climb stage, the fuel consumption of the smart morphing UAV is 11.47kg, representing a reduction by 0.02kg compared with the long-endurance UAV without smart morphing. The saved fuel can be used in the cruise stage to extend navigation. This shows that, in the climb stage, the use of smart morphing has a small effect on the climb rate. At the same time, as the climb altitude is only 7km, the fuel saved by the smart morphing throughout the whole climb stage is not obvious.

During the cruise stage, the fuel consumption per unit time (kg/h) of the UAV with and without smart morphing varies with the UAV weight as shown in Fig. 20. It can be seen that the average fuel consumption per unit time (kg/h) is reduced by 1.3% when adopting smart morphing. The endurance is calculated as follows, where E is calculated for every 20kg of fuel consumed:

$$E = \sum_{w_i=1004}^{W_f=749} \frac{20}{dW}. \quad \ldots (24)$$

The calculation results show that, with the 208kg available fuel, the endurance of the UAV without the smart morphing is 18.1h, while the endurance after adopting smart morphing is 18.85h. The endurance of the long-endurance UAV in the cruise stage increases by 3.7% in total when using the smart morphing method.

https://doi.org/10.1017/aer.2020.82 Published online by Cambridge University Press

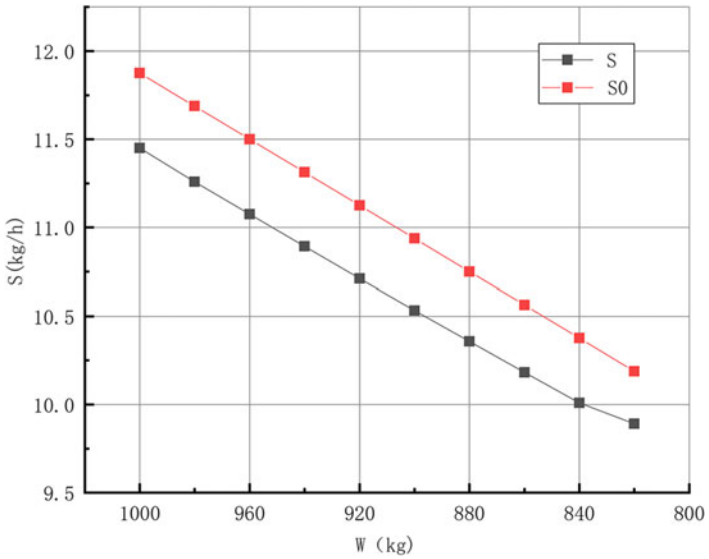

Figure 20. Change of the smart morphing long-endurance UAV fuel consumption rate (kg/h) with weight in the cruise stage compared with the long-endurance UAV without smart morphing.

6.0 CONCLUSIONS AND PROSPECTS

6.1 Conclusions

(1) To improve the endurance of long-endurance UAVs, a smart morphing method based on adjusting the wing shape and flight mode in real time is proposed. Based on this method, a smart morphing long-endurance UAV is designed.

(2) Focusing on the smart morphing control system design, an architecture for the smart morphing control system is proposed based on multi-agent theory, which is applicable to the complex smart morphing process. A workflow for the smart morphing control system is developed.

(3) For the morphing decision-making problem of the smart morphing control system, a morphing decision-making method is proposed based on the particle swarm optimisation algorithm, which can obtain the optimal wing shape and flight mode under the current environment with the goal of endurance improvement.

(4) The simulation results show that the morphing design meets the requirements of the smart morphing long-endurance UAV by improving its endurance. During the climb stage, with the same engine working condition, the smart morphing long-endurance UAV has little effect on the climb rate. As the climb altitude is only 7km, the fuel saving achieved by introducing smart morphing is not obvious in the climb stage. In the cruise stage, the average fuel consumption per unit time (kg/h) is reduced by 3.58% when using the smart morphing method. FOr the same total fuel consumption, the smart morphing method could improve the endurance by 4.1%. Even though this approach may cause a structural mass increase, the endurance improvement is significant.

https://doi.org/10.1017/aer.2020.82 Published online by Cambridge University Press

6.2 Prospects

The implementation of smart morphing technology in hardware still requires a lot of work. How to sense the wind field and the UAV's own status rapidly, how to resolve the morphing wing actuation problem under the precondition of not adding much structural weight and other issues still need further discussion. Regarding the presented approach, in the morphing decision-making method design part, further study is also needed on how to establish a model that is much closer to the true condition and how to make decisions more rapidly. Based on the results of this study, the smart morphing method has considerable application potential in the field of long-endurance UAVs. The improvement of the climb rate might have application potential in the field of near-space vehicles.

REFERENCES

1. LI, A., SHEN, Y. and ZHANG, W. The development of high altitude long-endurance UAV, *Aeronaut Sci Technol.*, 2001, **2**, pp 34–36.
2. BAI, P., CHEN, Q. and XU, G. Development status and prospect of key technologies of smart morphing aircraft, *Chin. J. Aero.*, June 2019, **37**, (3) pp 426–443.
3. XU, Y. Research on the development and key technologies of smart morphing, *Tactical Missile Technol.*, 2017, **2**, pp 26–33.
4. YIN, G., ZHU, T. and REN, P. Framework of electric vehicle chassis smart control system based on multi-Agent theory, *Chin. Mech. Eng.*, August 2018, **29**, (15), pp 1796–1801.
5. EBERHART, R. and KENNEDY, J. A new optimizer using particle swarm theory, Proceedings of the Sixth International Symposium on Micro Machine and Human Science, 1995. IEEE.
6. AN, L., LONG, T. and HUANG, B. Fast optimization design of long-endurance UAV airfoil based on particle swarm optimization, *J. Projectile Guid.*, June 2013, **33**, (3), pp 119–122.
7. ELZEY, D.M., SOFLA, A.Y.N. and WADLEY, H.N.G. A bio-inspired high-authority actuator for shape morphing structures, Smart Structures and Materials 2003: Active Materials: Behavior and Mechanics. International Society for Optics and Photonics, 2003.
8. WU R, *et al.* A morphing aerofoil with highly controllable aerodynamic performance. *Aeronaut. J.*, 2017, **121**, (1235), pp 54–72.
9. GUILER, R. and HUEBSCH, W. Wind tunnel analysis of a morphing swept wing tailless aircraft, AIAA: Applied Aerodynamics Conference, 2006.
10. HU, S. and ZHANG, L. The theory, technology and application of multi-agent system, *Comput. Sci.*, June 1999, **26**, (9), pp 20–24.
11. GUAN, X. and LI, Z. Research on aerodynamic shape CST parametric method, *Acta Aeronautica et Astronautica Sinica*, April 2012, **33**, (4), pp 625–633.
12. QIN, D., LI, Z. and WANG, X. ROTAX912/914 series aero-engine introduction, *Small Int. Combust. Eng. Veh. Technol.*, June 2017, **46**, (3), pp 92–96.
13. LIU, X. Flight Performance and Planning, 2013
14. ZHANG, Y., LUO, X. and XIANG, J. Calculation of flight range and flight time of propeller aircraft at constant altitude, *Flight Dyn.*, December 2003, **21**, (4), pp 30–34.
15. LI, H. *Design and Research of Long-Endurance Morphing UAV Based on Smart Materials*, 2016.
16. ANONYMOUS *Aeronautical Aerodynamic Manual*, National Defense Industry Press, 1990, pp 720–828.
17. VAN INGEN, J. The eN method for transition prediction. Historical review of work at TU Delft, 38th Fluid Dynamics Conference and Exhibit, 2008.

https://doi.org/10.1017/aer.2020.82 Published online by Cambridge University Press